Хаотические вихревые нити в конденсате Бозе - Энштейна и в сверхтекучем гелии.

Sergey K. Nemirovskii

Institute of Thermophysics,
Novosibirsk, Russia;

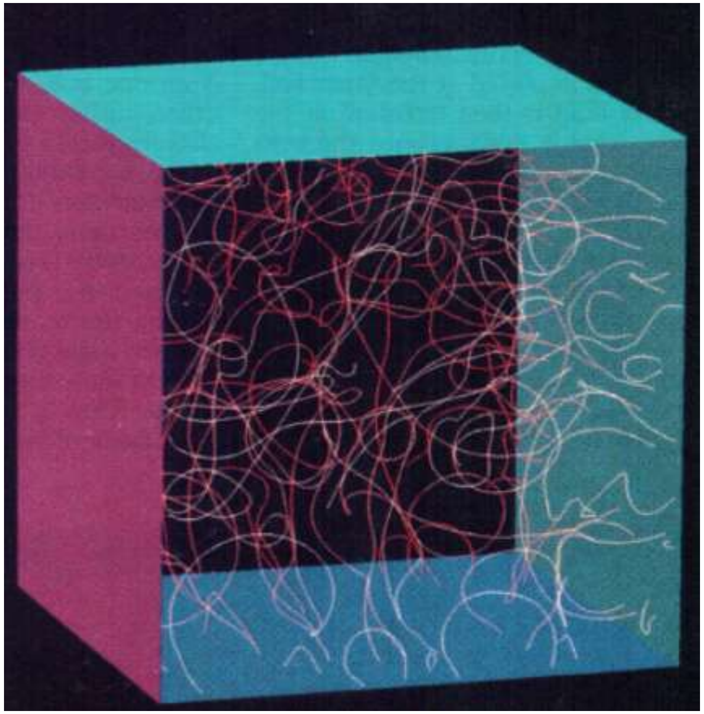

Two-fluid Landau model

From the viewpoint of hydrodynamics, He II can be viewed as a mixture of two components. One of them, a superfluid liquid with density $\rho_s(p, T)$ (p and T are the pressure and the temperature, correspondingly), moves with velocity $\mathbf{v}_s$. The superfluid component has no shear viscosity, and therefore it cannot be subjected to torsion $(\nabla \times \mathbf{v}_s = 0)$, and also cannot absorb and carry heat. From a deeper point of view, the flow of normal component is just the drift of the thermal excitations (phonons and rotons), which appeared in the background coherent state The motion of the two components is thermodynamically reversible and consequently independent. The superfluid component $\rho_s(T)$ appears at below $T_\lambda \approx 2.1768$ K at saturated vapor pressure, growing with the decrease of the temperature and reaching the full density $\rho = \rho_s(T) + \rho_n(T)$ at zero temperature.

component	velocity	density	viscosity	entropy
normal fluid	$\mathbf{v}_n$	ρ_n	η	s
superfluid	$\mathbf{v}_s$	ρ_s	0	0

Противоток (counterflow). Сверхтеплопроводность. Second sound (non statioanary counterflow), quench

$$\nabla \mu = \frac{1}{\rho}\nabla p - \frac{S}{\rho}\nabla T$$

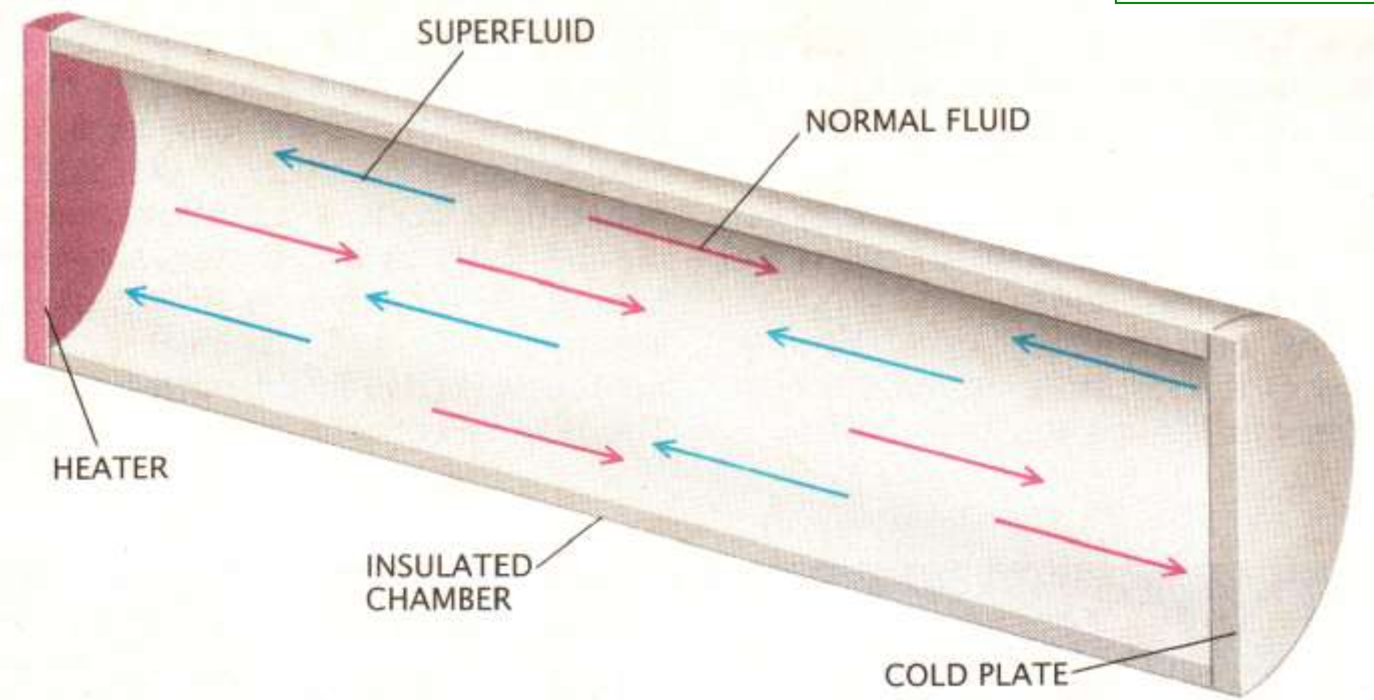

$$Q_{heat} = \frac{a^2 S^2 T}{8\eta}\nabla T$$

TWO-FLUID MODEL explains many properties of superfluid helium. According to this model, a sample of superfluid helium is made up of two interpenetrating fluids: a superfluid (*blue*), which flows without friction and, in one sense, has a temperature of absolute zero, and a normal fluid (*red*), which flows with normal friction and carries all the heat in the sample. A heater at one end of a channel of superfluid helium causes a counterflow: normal fluid "created" at the heater flows toward the other end of the channel while superfluid flows back in the opposite direction.

Парадокс вращения

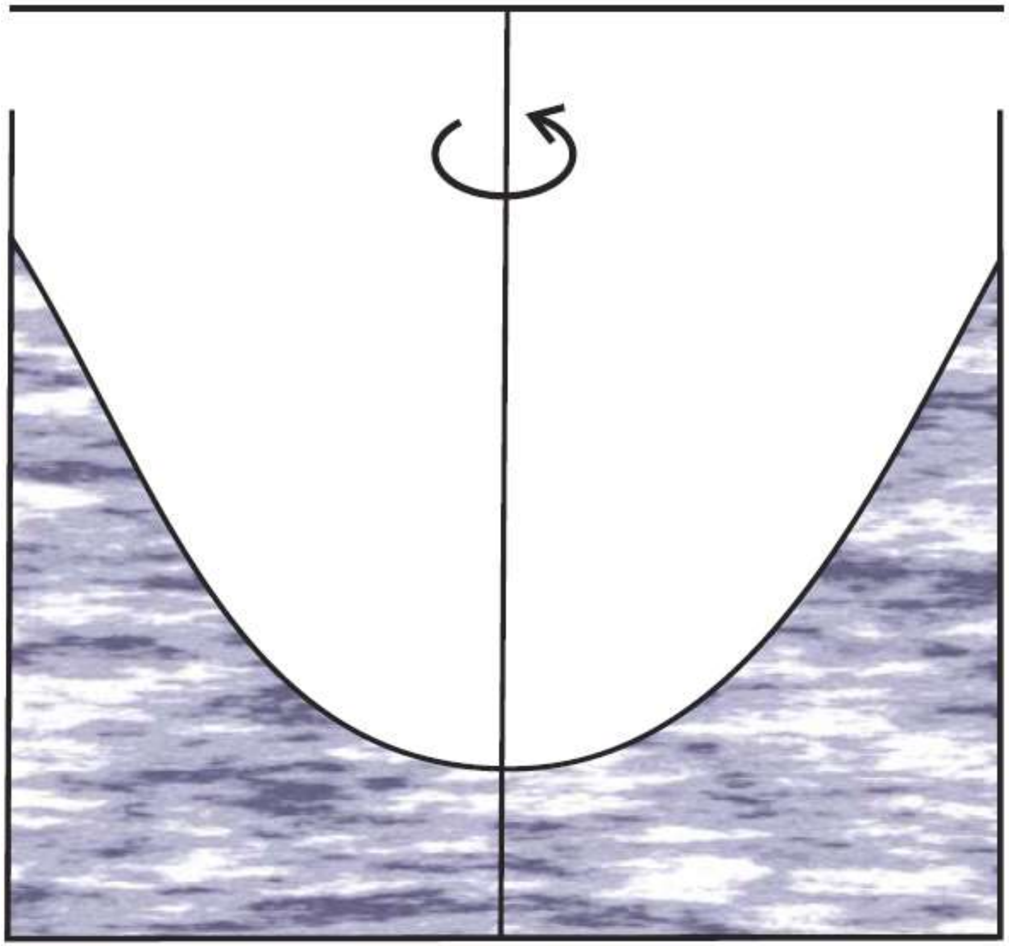

Квантовые вихри. Onsager, Feynman

Onsager
1903-1976

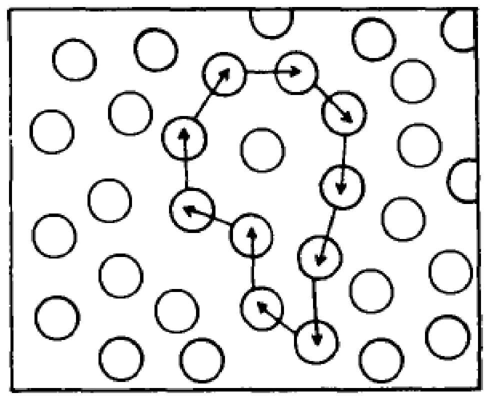

Fig. 5. The wave function must not change as a result of a permutation. If all the atoms are displaced around a ring, as shown, the phase change must be a multiple of 2π

R.P. Feynman: 1918-1988

Квантовые вихревые нити

$$\oint \mathbf{v}_s \cdot d\mathbf{l} = n\kappa.$$

$$\kappa = 2\pi\hbar/m_{He} = 9.97 \cdot 10^{-4}\ cm^2/s,$$

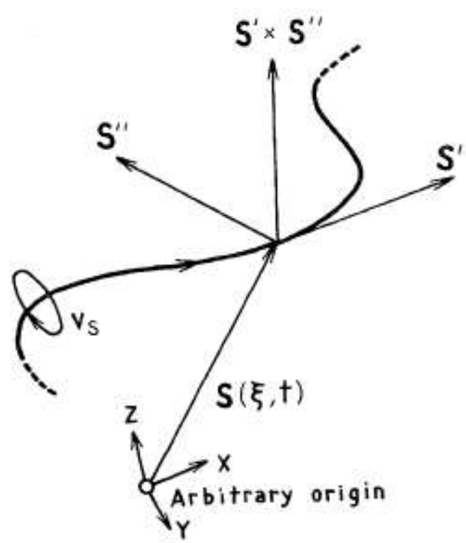

$$\mathbf{v}_s(\mathbf{r}) = (0, \frac{\kappa}{2\pi r}, 0)$$

Квантовые вихри. Onsager, Feynman

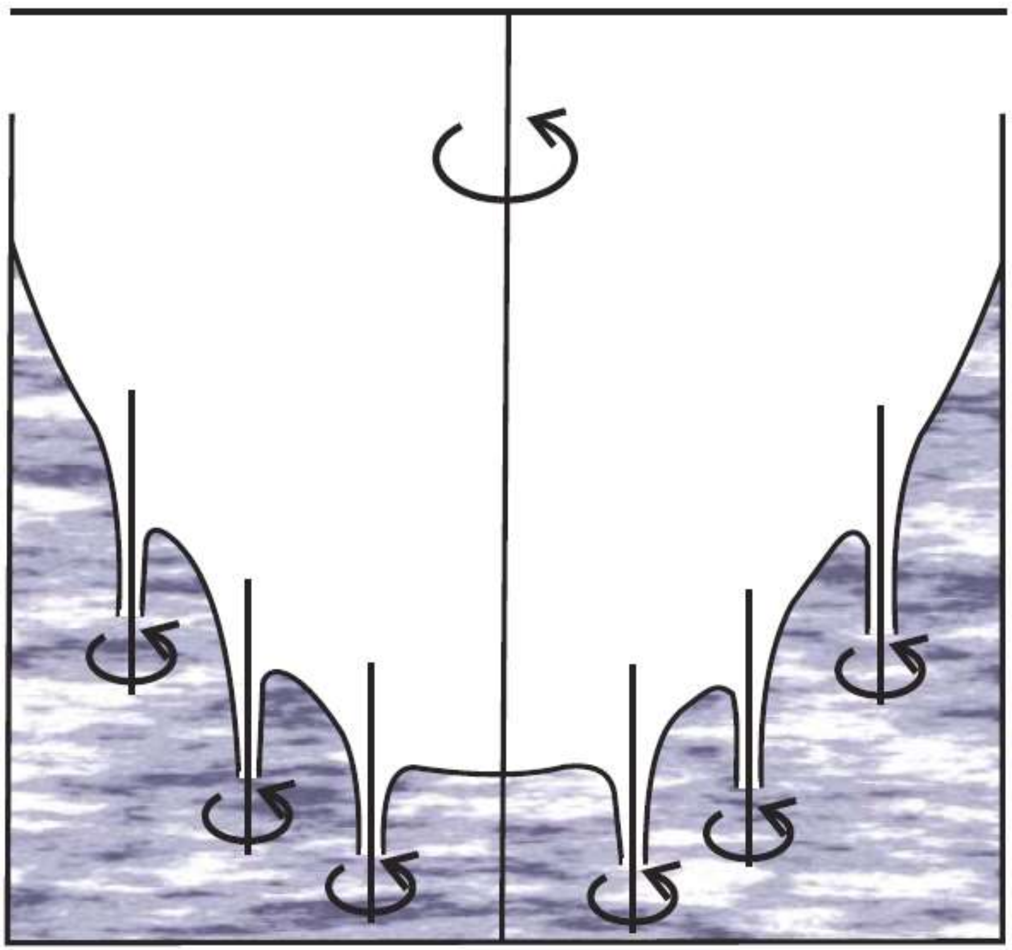

Клубок вихревых нитей. Квантовая турбулентность.

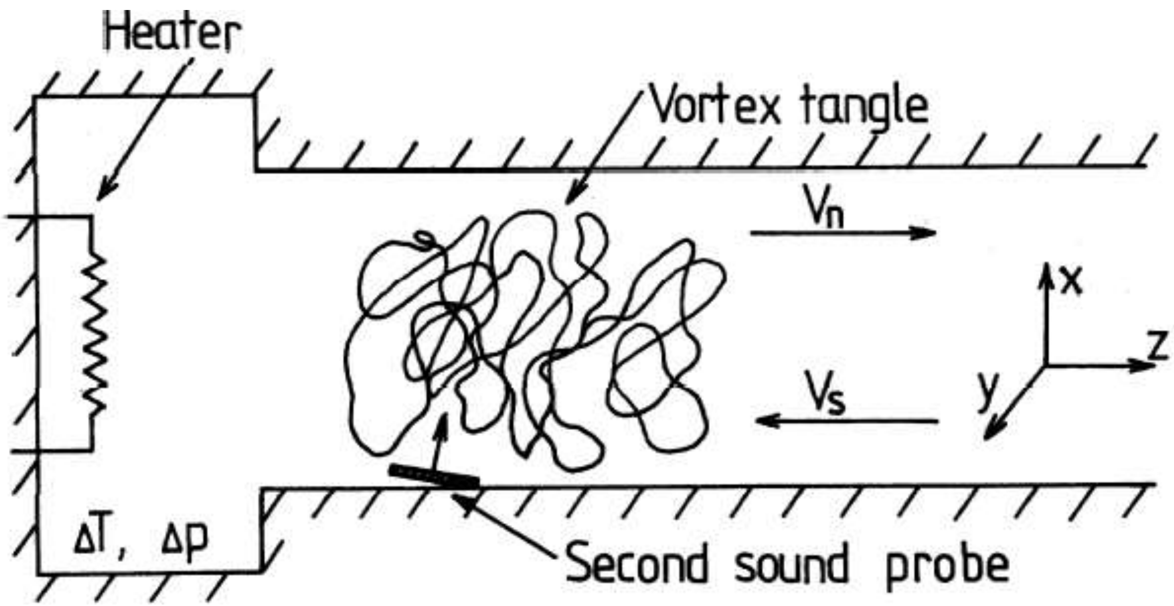

The vortices are the string-like 1D objects, their motion obey Bio-Savart law + interaction with normal component (mutual friction) + reconnection of lines.

$$\dot{\mathbf{s}} = \dot{\mathbf{s}}_i + \mathbf{v}_s + \alpha \mathbf{s}' \times (\mathbf{v}_{ns} - \dot{\mathbf{s}}_i) - \alpha' \mathbf{s}' \times \mathbf{s}' \times (\mathbf{v}_{ns} - \dot{\mathbf{s}}_i) + \mathbf{f}(\xi)$$

$$\dot{\mathbf{s}}_i(\xi, t) = \frac{\kappa}{4\pi} \int \frac{[\mathbf{s}(\xi', t) - \mathbf{s}(\xi, t)] \times \mathbf{s}'_{\xi'}}{|\mathbf{s}(\xi', t) - \mathbf{s}(\xi, t)|^3} d\xi'$$

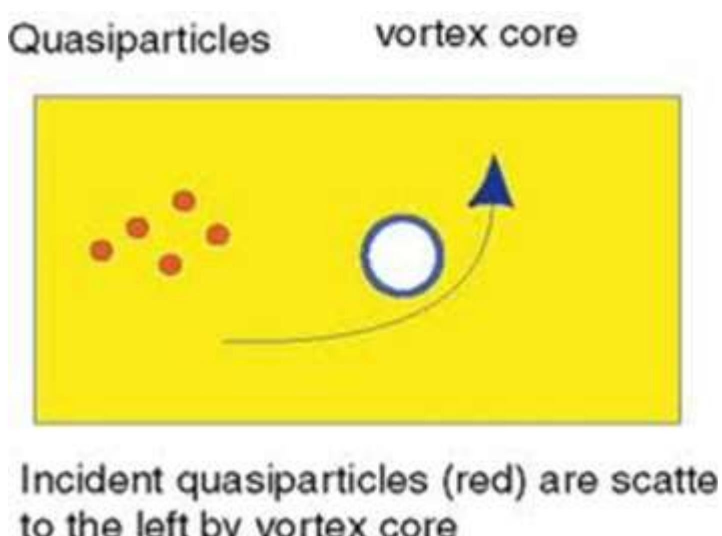

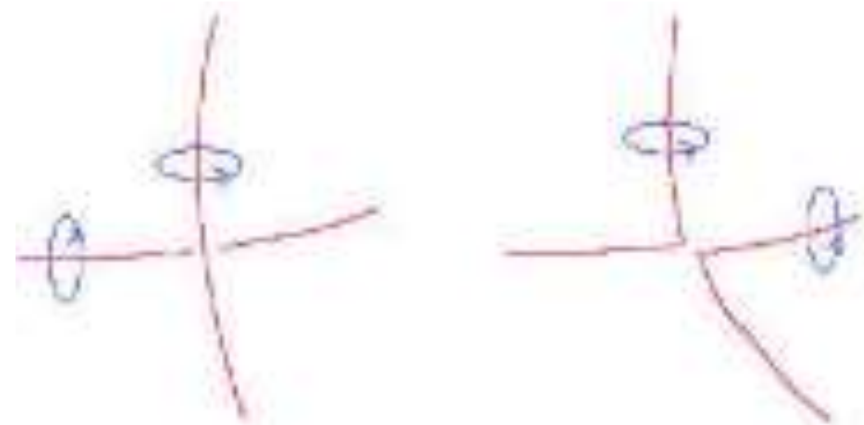

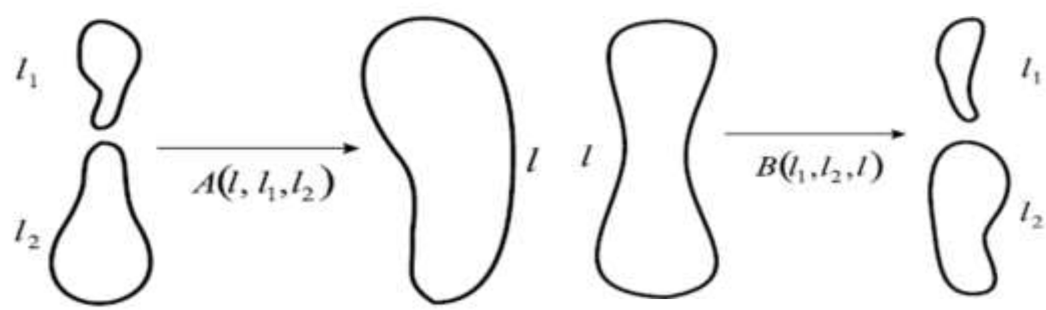

Feynman's qualitative model and Vinen phenomenological theory

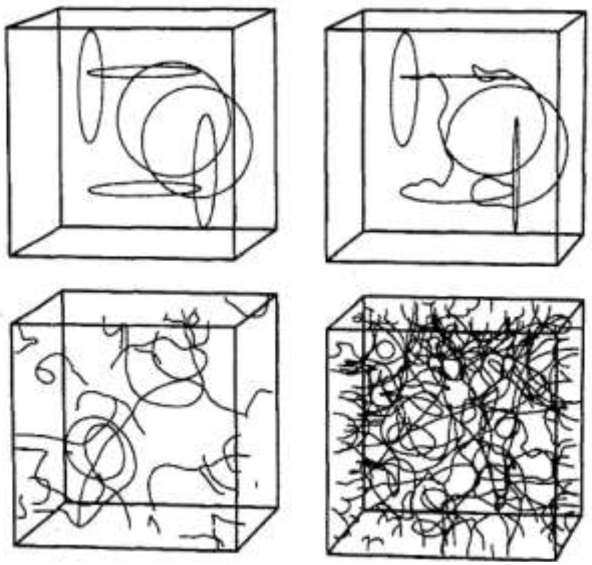

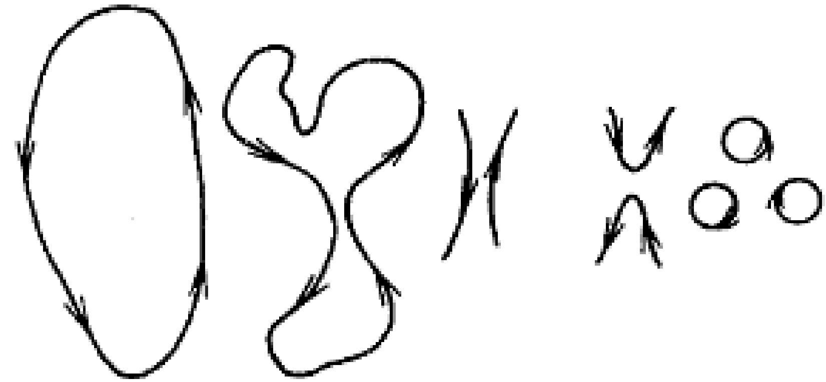

(a) (b) (c) (d) (e)

$$\frac{dL}{dt} = \alpha_V |\mathbf{v}_{ns}| L^{3/2} - \beta_V L^2 .$$

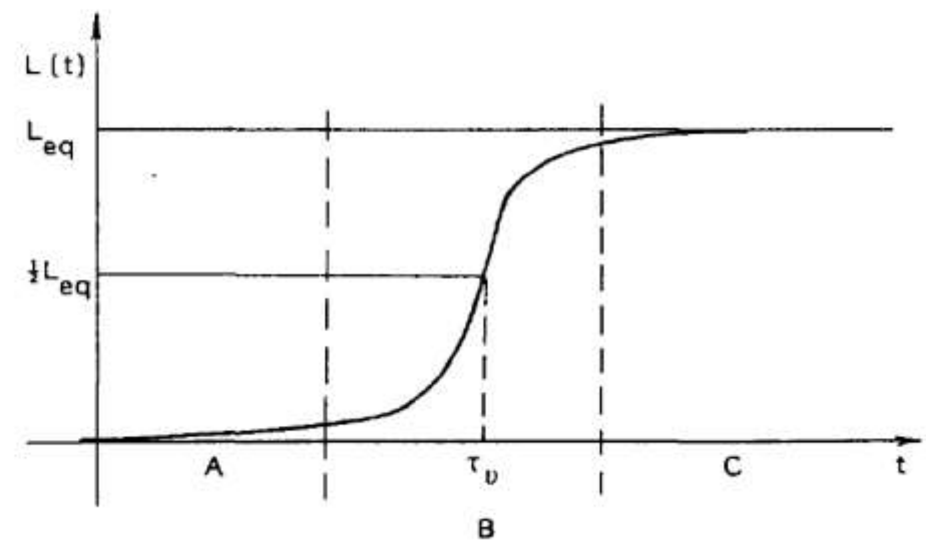

Figure 9 Possible shape of the function $L(t)$

Vortex Tangle in HeII. (K. Schwarz, 1988)

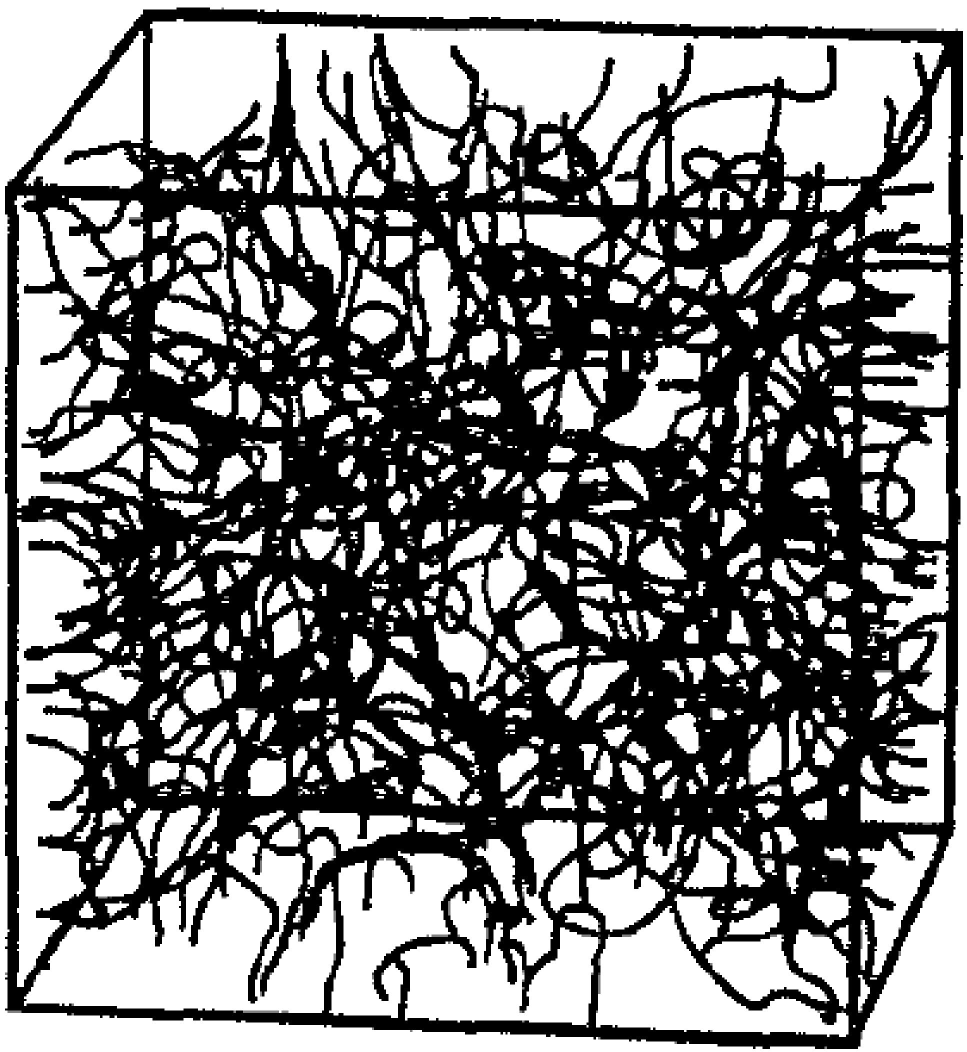

Numerical simulations

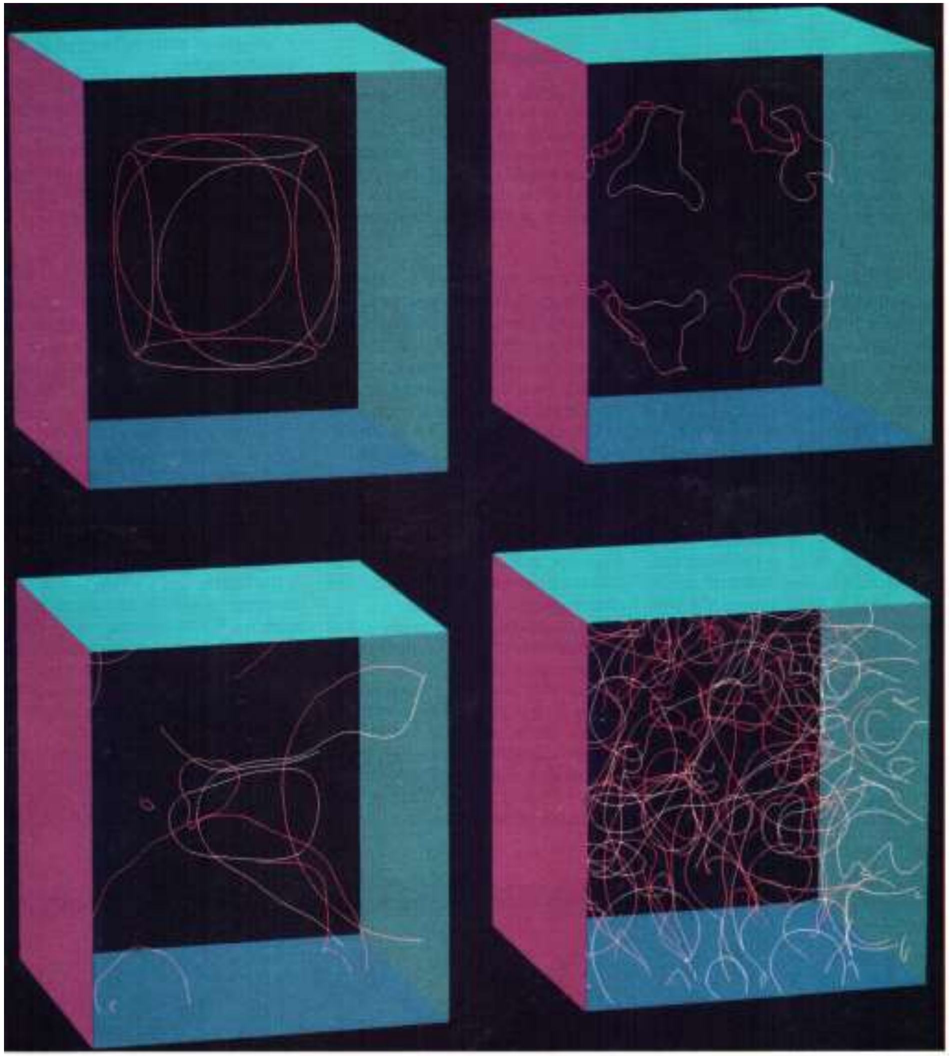

ONSET OF TURBULENCE in superfluid helium (a form of liquid helium that flows without viscosity or friction) is modeled in this computer-aided simulation created by Klaus W. Schwarz of the IBM Corporation's Thomas J. Watson Research Center in Yorktown Heights, N.Y. The thin red lines represent the cores of quantized vortices: vortices around which superfluid helium circulates at precisely determined speeds. At the beginning of the simulation (*top left*) the vortex cores are arranged in an orderly manner; each core is bent into a simple ring and the rings are positioned symmetrically. As the simulation evolves (*top right and bottom left*), the vortex cores twist and bend until finally they are snarled in a complex tangle (*bottom right*).

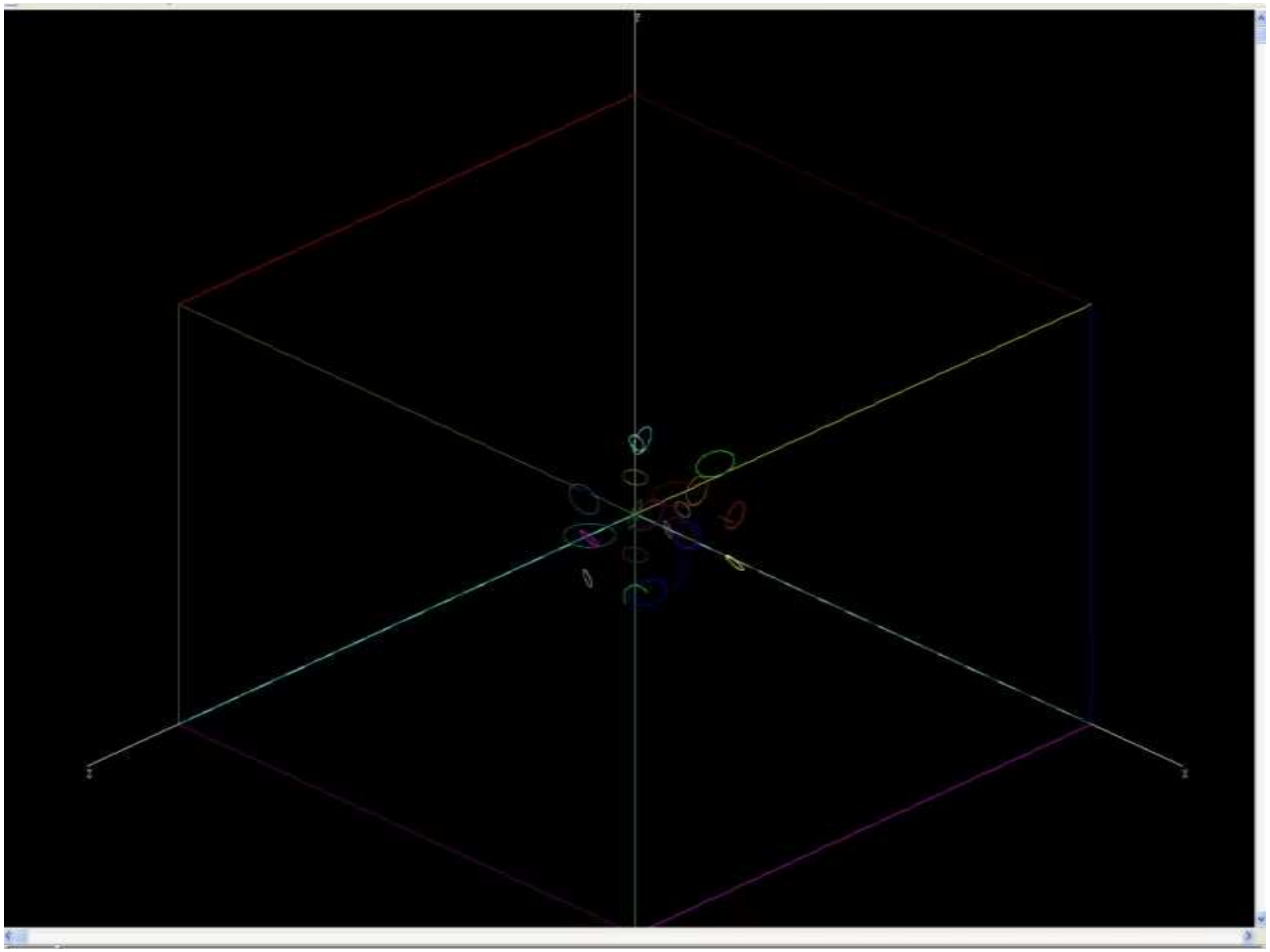

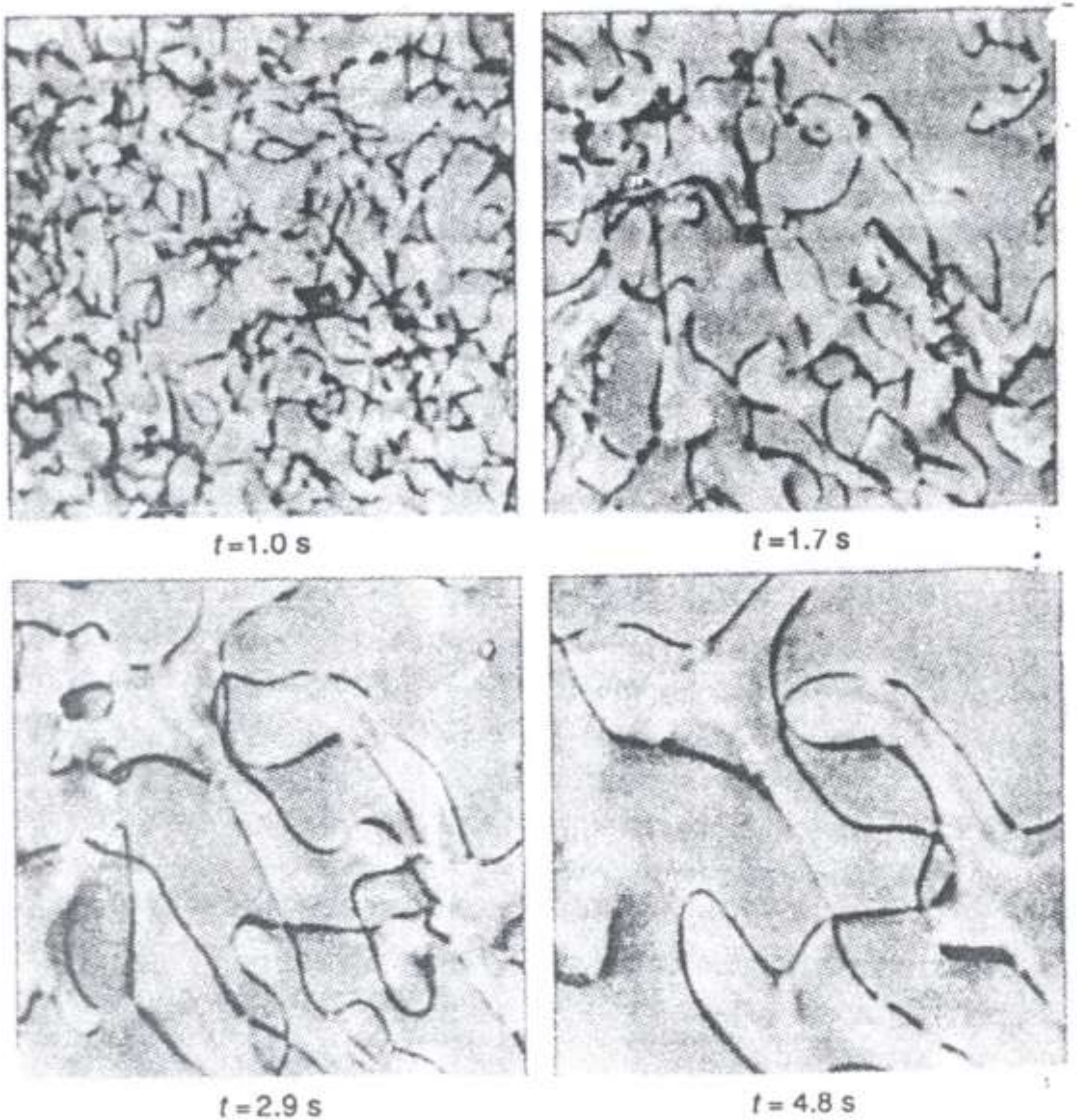

Fig. 4. A coarsening sequence showing the strings visible in our 230-µm-thick pressure cell containing K15 nematic liquid crystal, at t = 1.0, 1.7, 2.9, and 4.8 seconds after a pressure jump of ΔP = 4.7 MPa from an initially isotropic state in equilibrium at approximately 33°C and 3.6 MPa. The evolution of the string network shows self-similar or "scaling" behavior. Each picture shows a region 360 µm in width.

Tangle of string-like defects in nematic liquid crystal

I.Chuang, R. Durrer, N. Turok, B. Yorke, ("Science", 1991)

Dislocations in solids,
C. Deeb et al. (2004)

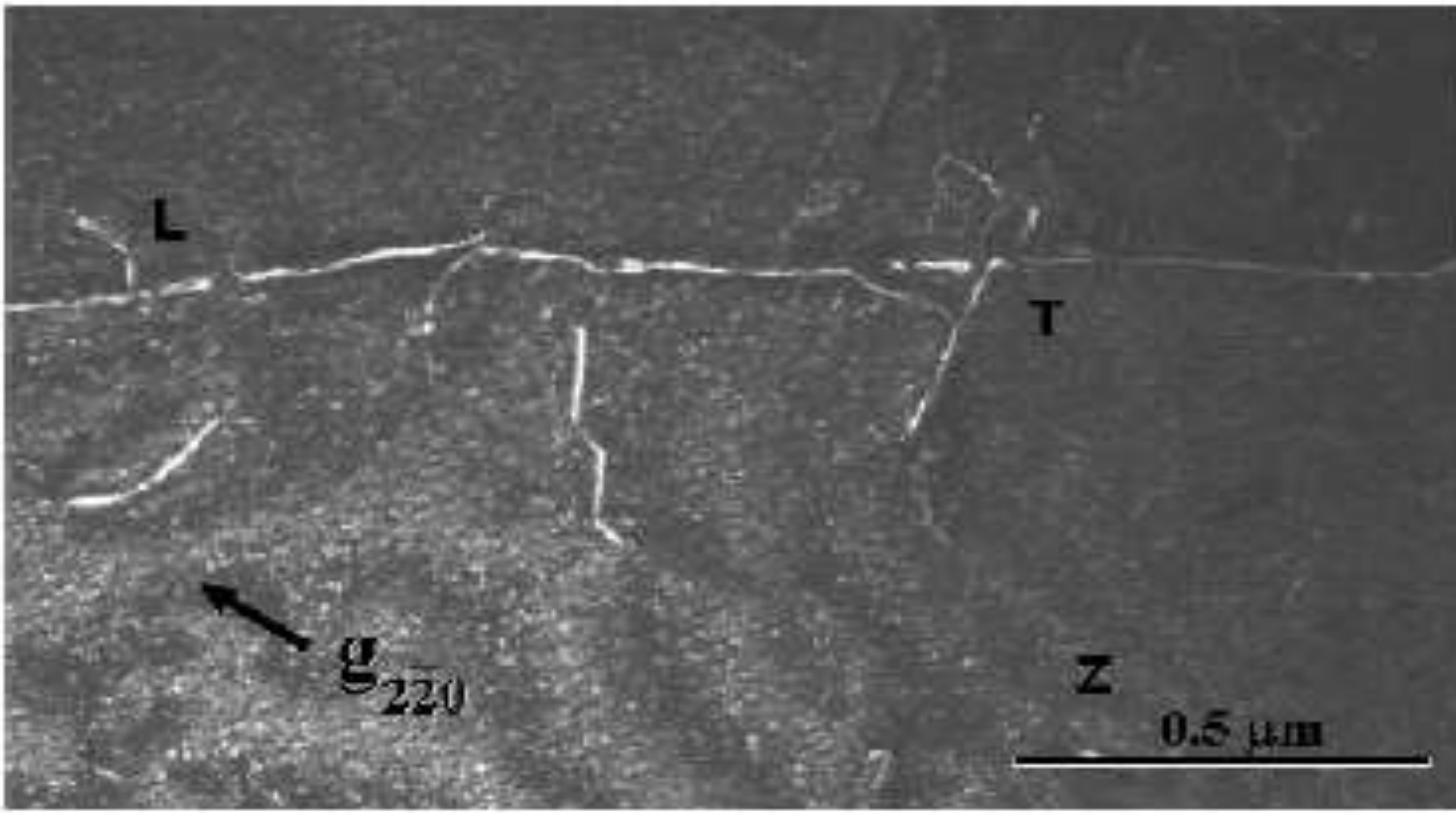

Network of cosmic strings (D. Bennet, F. Bouchet,1989)

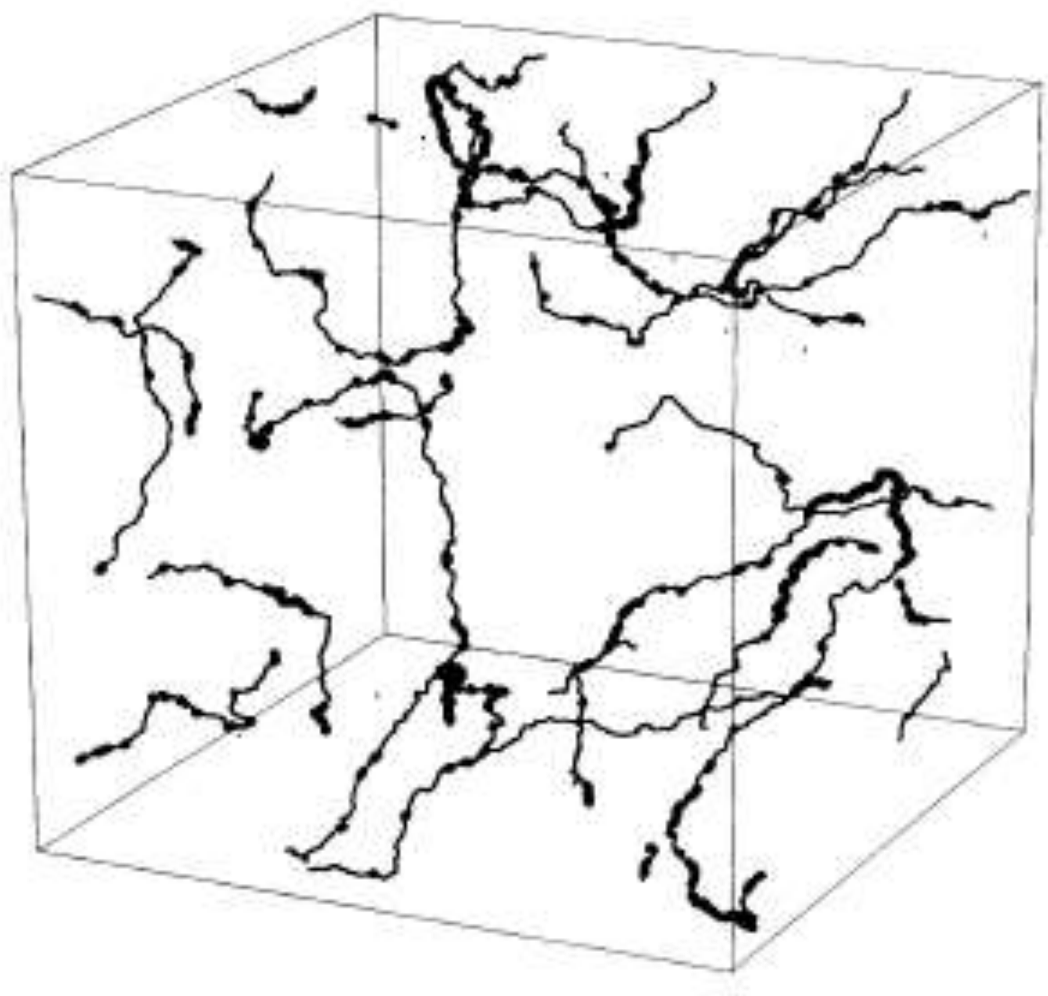

Fractality of Light's Darkness

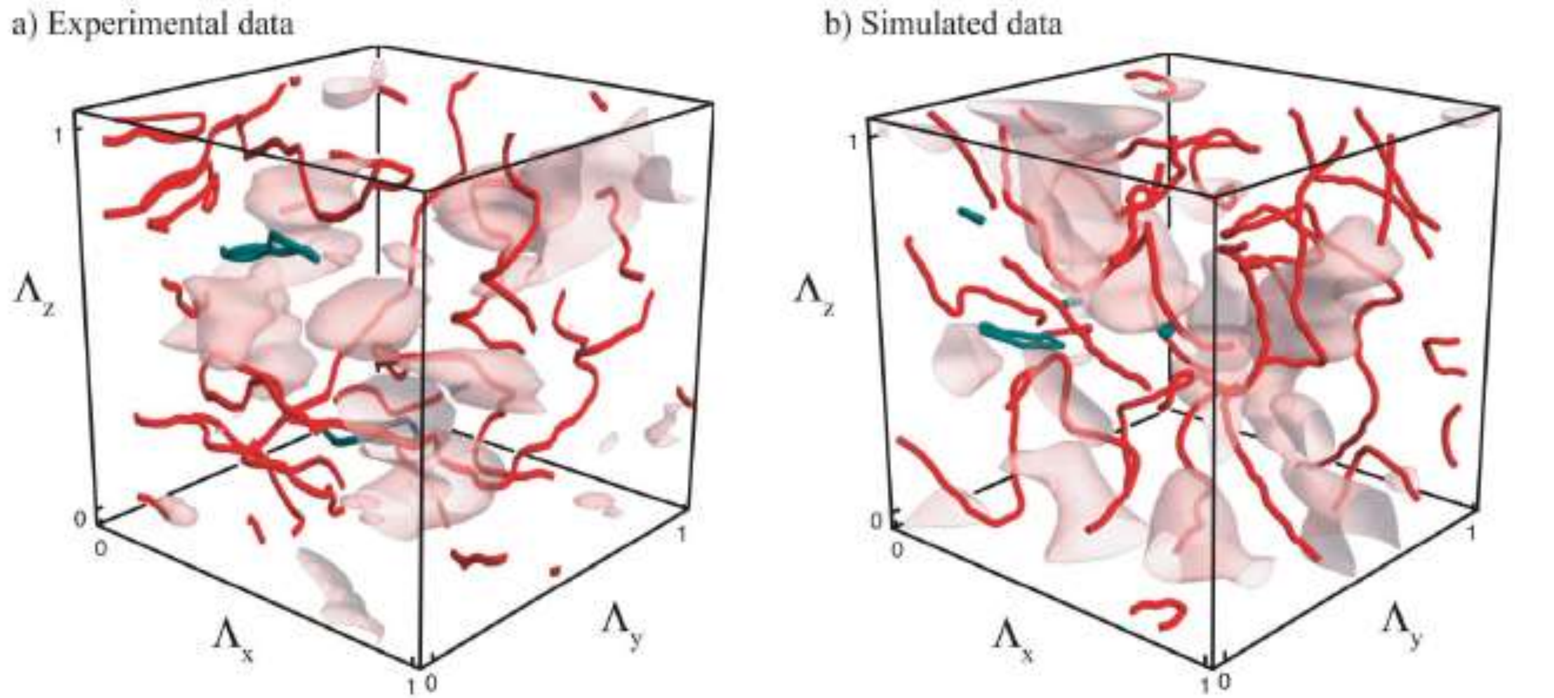

FIG. 1 (color online). Vortex structure in speckle: (a) experimental vortex structure obtained through interferometric measurements of laser speckle created by the scattering of a 10 mm diameter HeNe laser beam through a ground glass screen and (b) numerical simulation of the vortex structure from Gaussian random wave superposition. The open vortex lines are plotted in red and the closed loops in dark green. Surfaces of 50% maximum intensity are also shown. Both are plotted over one natural volume of the speckle, $\Lambda_x \times \Lambda_y \times \Lambda_z$. Although different in detail, the two patterns have similar characteristics.

Tangle of vortex filaments obtained in turbulent flow at moderately high Reynolds (Vincent and Meneguzzi 1991).

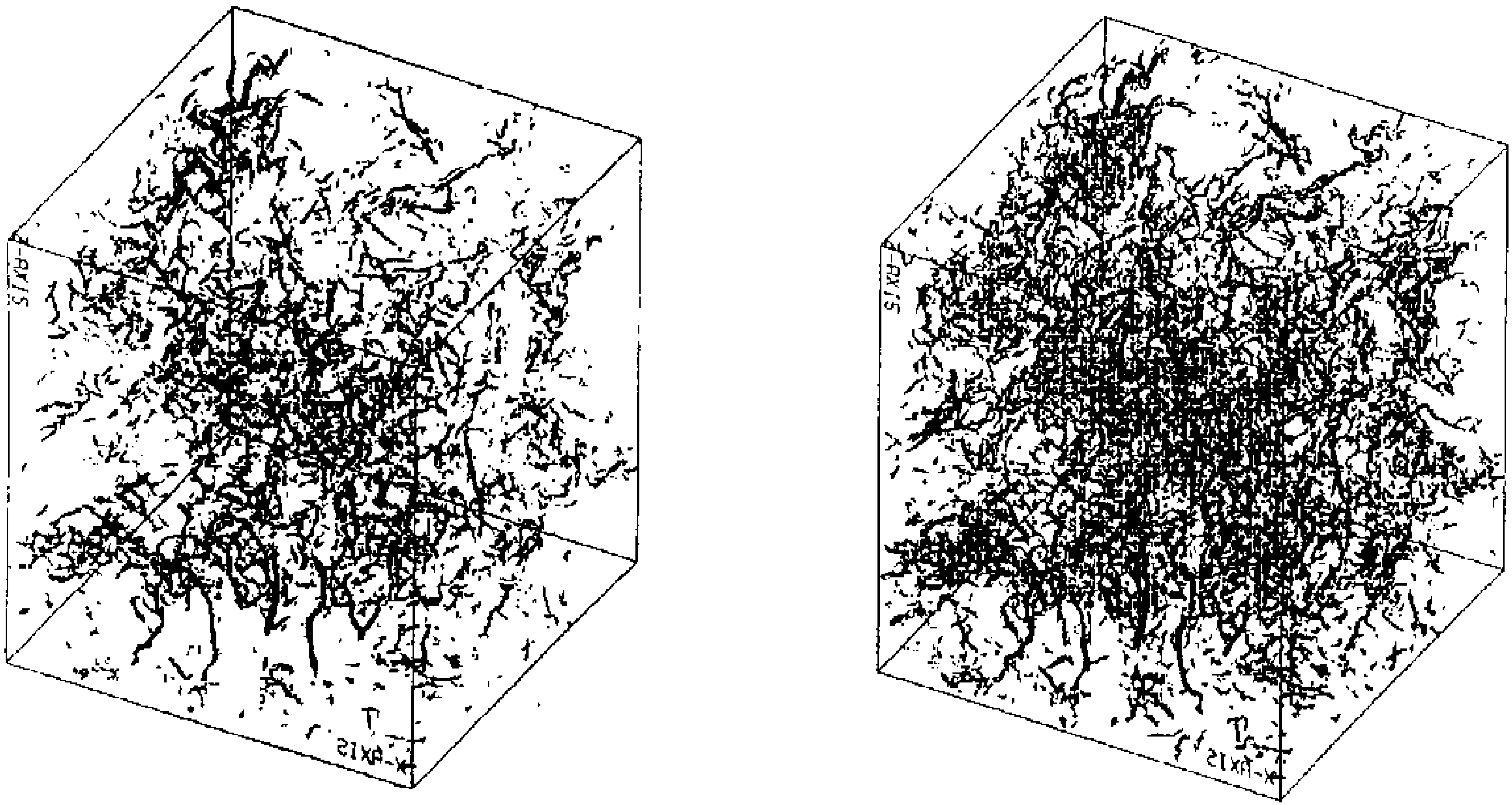

(a) (b)

Filamentary structure of classical turbulence

Idea of modeling turbulence by discrete vortices on experimental and numerical evidences of that the developed turbulence has the vortex filamentary structure.

A. Vincent and M. Meneguzzi, Journal of Fluid Mechanics **225**, 1 (1991).

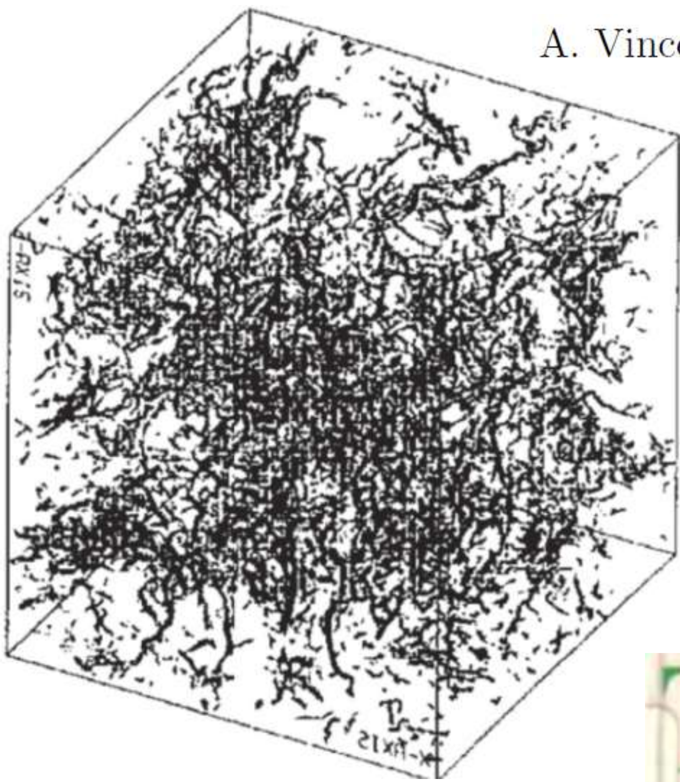

8.9.2 Statistical signature of vortex filaments: dog or tail?

Gross–Pitaevskii equation (GPE).

$$i\hbar \frac{\partial \psi}{\partial t} = \frac{\hbar^2}{2m} \Delta \psi + U_0 \left(|\psi|^2 - n \right) \psi$$

$$\psi(\mathbf{r}, t) = \sqrt{\rho(\mathbf{r}, t)/m} \exp(i\phi(\mathbf{r}, t)) \qquad \mathbf{v} = \frac{\hbar}{m} \nabla \phi.$$

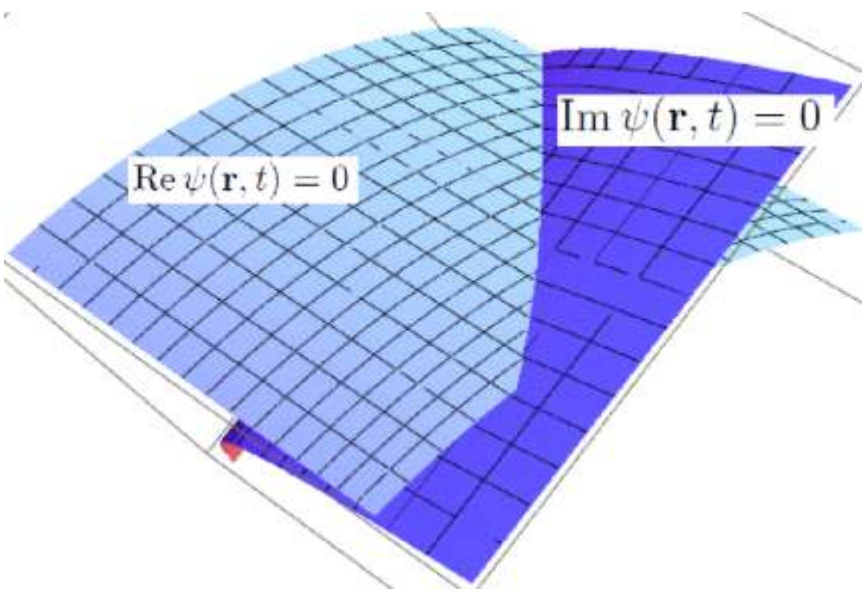

Topological defects in Bose Gas (N. Berloff, B. Svistunov, 2001)

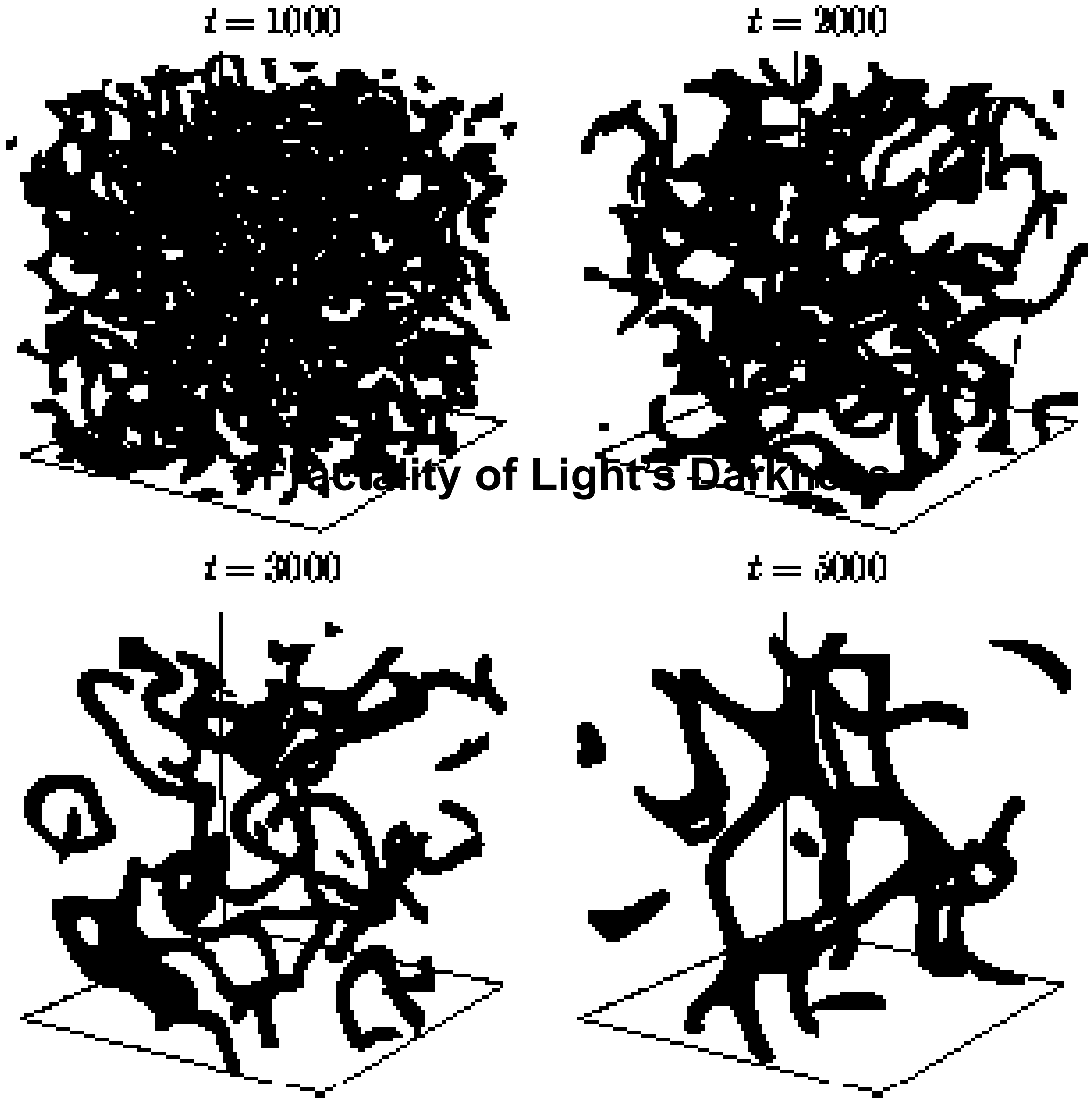

Fractality of Light's Darkness

Quantum Turbulence in BEC

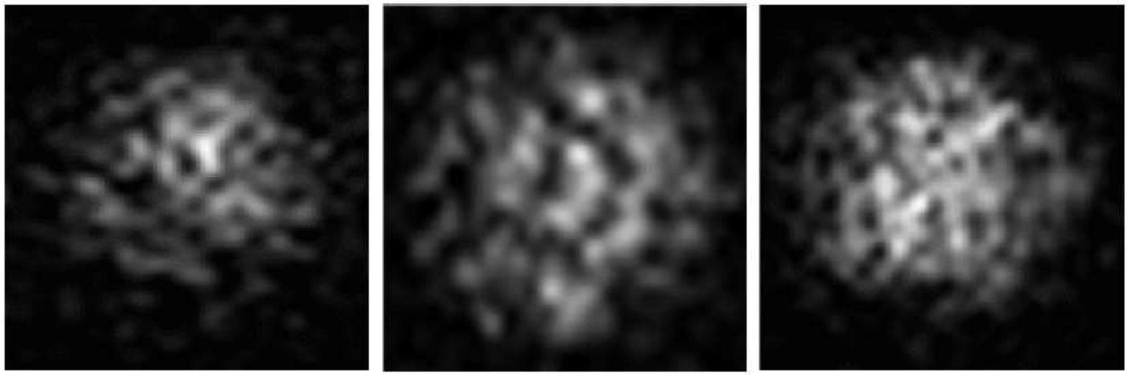

Fig. 4 (Color online) Vortex turbulence. Cross-section of a random vortex tangle obtained by numerical simulations. Darker coulor corresponds to lower density, thus vortices are shown as black spots.

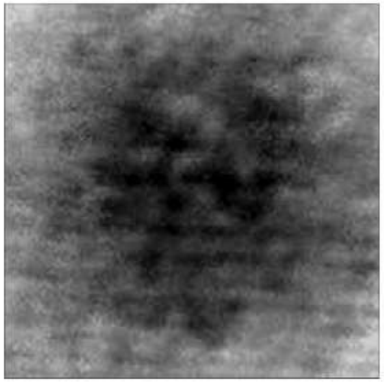

Fig. 5 (Color online) Vortex turbulence. Experimental observation of a vortex turbulent state in the cloud ^{87}Rb atoms. Multiple dark spots correspond to vortices.

QT in Helium vs QT in BEC

- Because of absence of the rigorous microscopic theory in He II, results concerning vortices in superfluid helium bear phenomenological character. It concerns equation of motion, structure of core, reconnection procedure etc. Therefore there exist various “artifical” prescriptions like “reconnection ansatz”.
- Unlike this, the laws of dynamics for vortices in BEC are based on the GPE. Therefore many of listed problems have strict solutions, which widely used for interpretations of similar phenomena in superfluid helium.
- Experiment

Advantage and limitations of GPE method

They are not string-like objects, they are rather thick tubes.

$$\text{sound velocity} = \frac{\kappa}{\sqrt{2}\, a_0}$$

BEC is not noncompressible fluid, this radically changes all turbulent phenomena (energy flux, spectra, decay etc.)

Computational costs (N number of disretization).

N^3	$N \ln N$
BEC	strings-like, filament vortices

Неоднородность, малое количество атомов

Thank you for your attention

Visualization of the vortex lines

50 years on…

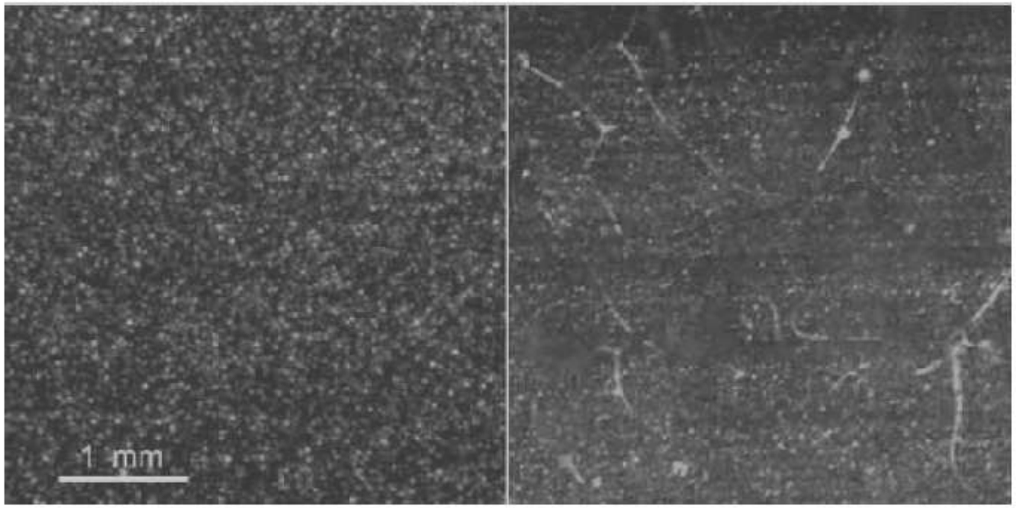

~50 mK above T_λ   **~50 mK below T_λ**

The left panel shows a suspension of hydrogen particles just above the transition temperature. The right panel shows similar hydrogen particles after the fluid was cooled below the lambda point. Some particles have collected along filaments, while other are randomly distributed as before. Fewer free particles are apparent on the right only because the light intensity was reduced to highlight the brighter filaments in the image. Volume fraction $\cong 3\text{X}10^{-5}$.

G.P. Bewley, D.P. Lathrop & KRS, Nature 441, 558 (2006)

Реконнекция, визуализация.

Dynamics of heat pulses

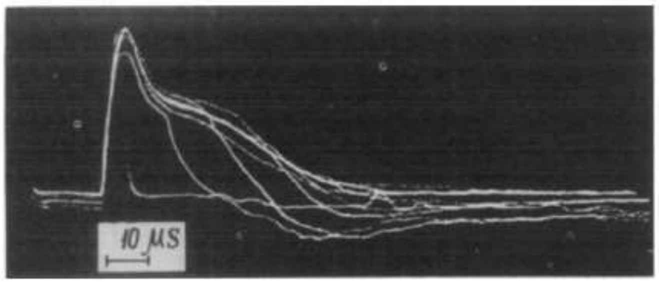

Figure 3 Appearance of the limiting profile of a second sound pulse as t_S increases: $t_S = 3$, 18, 30, 40, 50, 60, and 70 μs. $W = 73.5$ W cm^{-2}, $T = 1.884$ K[23]

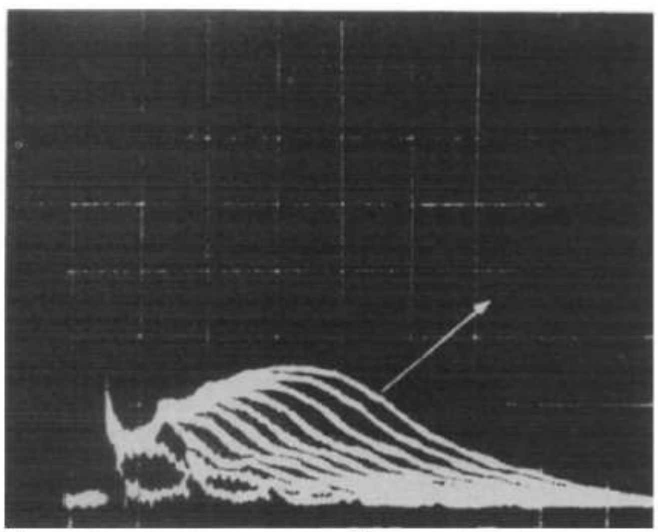

Figure 4 Secondary temperature fronts produced by heat pulses in the presence of the vortex tangle. Oscillographs show temperature *versus* time (10 ms/div.). Arrow indicates how temperature profiles progressively develop as *W* increases. At the very beginning of the oscillographs, there are second sound shock waves[18]

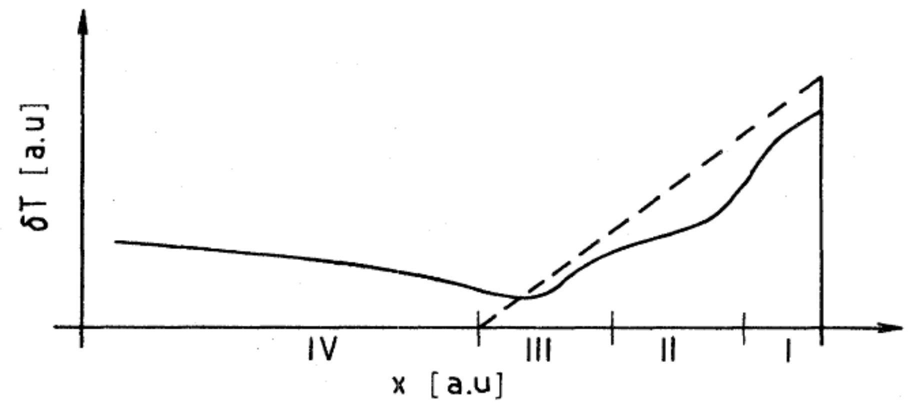

FIG. 28. Schematic of the distortion of the temperature pulse due to the interaction with is "own " vortex lines (Nemirovskii and Schmidt, 1990, Fig. 7). The dashed line represents the vortexless case when the pulse should be a "Burgers" triangle.

Illustration to reconnection

Реконнекция (изменение топологии)

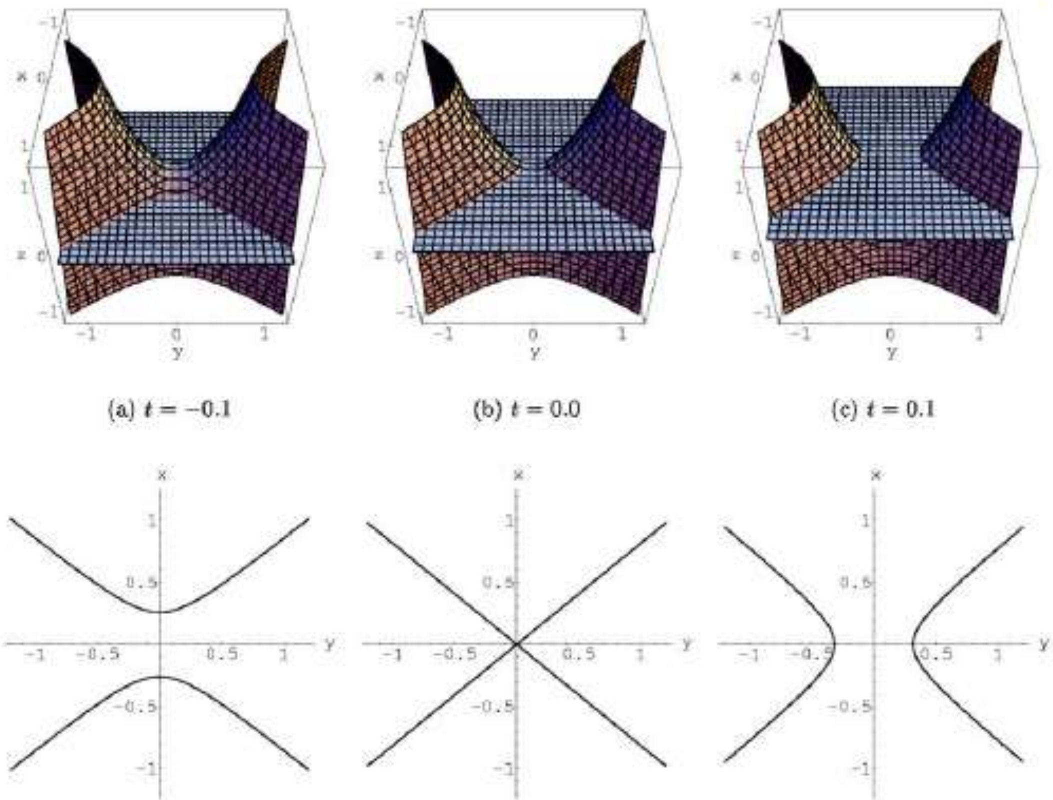

(a) $t = -0.1$ (b) $t = 0.0$ (c) $t = 0.1$

(d) $t = -0.1$ (e) $t = 0.0$ (f) $t = 0.1$

S.V. Nazarenko and R.J. West Analytical solution for nonlinear Schrodinger vortex reconnection // J. Low Temp. Phys, 132 (1-2): 1-10 JUL 2003.

Quantum Turbulence in BEC